

# Significantly enhancing the biocatalytic synthesis of chiral alcohols by semi-rationally engineering an anti-Prelog carbonyl reductase from *Acetobacter* sp. CCTCC M209061



Ping Wei<sup>a,b,1</sup>, Ze-Wang Guo<sup>a,1</sup>, Xiao-Ling Wu<sup>a</sup>, Shan Liang<sup>a</sup>, Xiao-Yang Ou<sup>a</sup>, Pei Xu<sup>a</sup>, Min-Hua Zong<sup>a</sup>, Ji-Guo Yang<sup>c</sup>, Wen-Yong Lou<sup>a,c,\*</sup>

<sup>a</sup> Lab of Applied Biocatalysis, School of Food Science and Engineering, South China University of Technology, Guangzhou 510641, China

<sup>b</sup> School of Biotechnology and Health Sciences, Wuyi University, Jiangmen 529020, China

<sup>c</sup> Innovation Center of Bioactive Molecule Development and Application, South China Institute of Collaborative Innovation, Dongguan 221116, China

## ARTICLE INFO

### Keywords:

Carbonyl reductase  
Asymmetric reduction  
Semi-rational design  
Chiral alcohols

## ABSTRACT

Chiral alcohols and their derivatives are vital building blocks to synthesize pharmaceutical drugs and high-valued chemicals. Wild-type carbonyl reductase AcCR from *Acetobacter* sp. has ideal enantioselectivity toward 11 prochiral substrates (*e.e.* > 99%) but poor activity. In this work, a semi-rational engineering was performed to enhance the activity of AcCR. Fortunately, three positive double-mutants (mut-E144A/G152L, mut-G152L/Y189N, and mut-I147V/G152L) with specific activity 17–61 folds higher than that of enzyme without modified were achieved. Kinetic studies suggested that the catalytic efficiencies ( $k_{cat}/K_m$ ) of these mutants were also well enhanced. Finally, these modified mut-AcCRs were successfully applied in asymmetric reductions of 11 structurally diverse prochiral substrates (200 mM) with excellent product yields (76.8%–99.1%) and enantiomeric excess (*e.e.* > 99%), which provides an alternative strategy for efficient synthesis of chiral alcohols for pharmaceuticals industry with ideal yield and enantioselectivity.

## 1. Introduction

Chiral alcohols and their derivatives are important building blocks that have been widely used in synthesis of various vital chiral chemicals such as chiral pharmaceuticals, flavors, liquid crystals and biointerface materials [1–3]. Currently, biosynthesis relies on the enzymes and whole-cells has been an alternative for production of chiral alcohols [4–7]. Compared to chemical synthesis, enantioselective carbonyl compound reductions are reliable, green and straightforward routes to obtain optically active alcohols [8–10].

Carbonyl reductase (EC 1.1.1.148) as efficient oxidoreductase has been proved to be powerful biocatalysts for the asymmetric reduction of carbonyl substrates to the synthesis of chiral alcohols [11–14]. However, two major challenges restricted the efficiency of biocatalytic redox reductions of carbonyl reductases for their applications in asymmetric synthesis. First, most of the interesting substrates are insoluble or poorly soluble in the natural enzyme-containing aqueous phase. This disadvantage has been effectively conquered by using non-aqueous media like ionic liquids, organic solvents and supercritical

carbon dioxide in biphasic systems [15,16]. The second challenge is the limited activities of most carbonyl reductases confined by substrate specificity, coenzyme dependence and elasticity of physiological environment, resulting in the lack of an appointed asymmetric reduction efficiency [17–19]. For example, an (*S*)-carbonyl reductase from *Candida parapsilosis* is only capable to catalyze the reduction of 2-hydroxy-1-phenylethanone to (*S*)-1-phenyl-1,2-ethanediol at the conditions of pH 6.5 and 30 °C [20–23]. Additionally, a carbonyl reductase (NcCR) from *Neurospora crassa* showed strict substrate specificity to many kinds of ketones, with 468 U/mg activity being confirmed in reduction of dihydroxyacetone. However, the enantioselectivity of NcCR for reduction of ethyl 4-chloro-3-oxobutanoate strongly depended on temperature, revealing that the product *e.e.* value could be dramatically decreased by increasing the temperature from –3 °C to 40 °C (98.0% vs 78.8%) [24].

To improve the performance of the carbonyl reductases, various enzymes have been successfully modified by using random mutagenesis and rational design to improve operational stability, expand the range of substrate spectrum, and improve regio-and/orstereo-selectivity

\* Corresponding author at: Lab of Applied Biocatalysis, School of Food Science and Engineering, South China University of Technology, Guangzhou 510641, China.  
E-mail address: [wylou@scut.edu.cn](mailto:wylou@scut.edu.cn) (W.-Y. Lou).

<sup>1</sup> These authors contributed equally to this work.

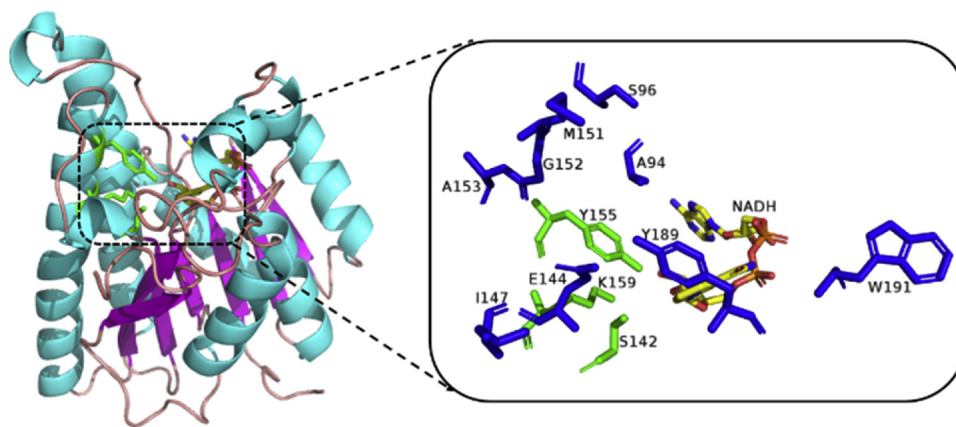


Fig. 1. Catalytic triad and mutation sites.

**Table 1**  
Enzyme activity of different AcCR mutants.

Enzyme	4'-Chloroacetophenone (1a)		Ethyl 2-oxo-4-phenylbutyrate (2a)		2-Hydroxy-1-phenylethanone (3a)	
	Enzyme activity [U/mg] <sup>a</sup>	Fold change <sup>b</sup>	Enzyme activity [U/mg] <sup>a</sup>	Fold change <sup>b</sup>	Enzyme activity [U/mg] <sup>a</sup>	Fold change <sup>b</sup>
AcCR	5.17	1.00	1.45	1.00	0.37	1.00
A94Q	4.07	0.79	2.73	1.88	0.27	0.73
S96Y	5.22	1.01	1.61	1.11	0.42	1.13
S96T	5.99	1.16	1.67	1.15	0.34	0.90
E144A	47.24	9.14	0.90	0.62	0.28	0.74
I147V	5.05	0.98	5.98	3.62	1.76	4.71
M151T	5.69	1.10	1.91	1.31	1.90	5.06
G152L	23.19	4.49	5.82	4.01	4.33	11.56
G152A	6.92	1.34	4.50	3.10	0.83	2.22
G152C	5.79	1.12	4.25	2.93	0.15	0.40
Y189N	2.03	0.39	73.44	50.58	0.12	0.33
W191A	2.98	0.58	5.39	3.72	1.37	3.66

<sup>a</sup> 0.25 mM NADH, citrate-phosphate buffer (pH 6.5, 50 mM), and 5 mM 1a or 2a or 3a were incubated for 5 min at 35 °C followed by adding a certain amount of purified enzyme, the changes in absorbance after 3 min were recorded.

<sup>b</sup> Fold change improvement in enzyme activity over the WT enzyme.

[25–29]. For example, a carbonyl reductase from *Ogataea minuta* with improved thermostability was achieved by directed evolution strategy. As a result, in the absence and presence of 20% (v/v) dimethyl sulfide, the half-lives of mutant-V166A were 6.1 and 11 times longer than those of the wild type one at 50 °C, respectively [30]. Additionally, activity improvement of *Kluyveromyces lactis* aldo-keto reductase *KIAKR* was carried out via rational design. On the basis of homology modeling and molecular docking, mutant *KIAKR*-Y295W/W296L showed the highest catalytic efficiency ( $k_{cat}/K_m$ ) *tert*-butyl 6-cyano-(5*R*)-hydroxy-3-oxohexanoate, the  $k_{cat}/K_m$  was up to  $12.37 \text{ s}^{-1} \text{ mM}^{-1}$ , which was 12.5 folds higher than that of the wild type one, showing that the efficient activity improvement of *KIAKR* was realized through rational design successfully [31]. Therefore, protein engineering as a kind of powerful tool for tailoring enzymes could significantly improve the performance of the biocatalyst.

In our previous work, a versatile anti-Prelog carbonyl reductase AcCR discovered from *Acetobacter* sp. CCTCC M209061 was characterized, proving that the enzyme was able to catalyze the asymmetric reduction of various carbonyl substrates with excellent stereoselectivity, including acetophenone derivatives and aliphatic ketone ester. However, the specific activity of AcCR to reduction of ethyl 2-oxo-4-phenylbutyrate (2a) (1.5 U/mg) and 2-hydroxy-1-phenylethanone (3a) (0.4 U/mg), which are useful chiral building blocks, were

unsatisfactory [32–34]. Therefore, a semi-rational design based on the combination of homology modelling and saturation site-directed mutagenesis was applied for the modification of AcCR. Apparent kinetic parameter and docking experiments were used to illustrate the mechanism of the changes in enzyme characteristics. Finally, three positive double-mutants were obtained with excellent product yields (76.8%–99.1%) and enantiomeric excess (*e.e.* > 99%), suggesting its potential application to product the pharmaceutically relevant chiral alcohols.

## 2. Experimental

### 2.1. Chemicals, plasmids and strains

BL21(DE3) (Novagen, Darmstadt, Germany) was as the host cell, and pGEX plasmid was used for cloning and expression. BL21(DE3)/pGEX-AcCR was used to express AcCR. PrimeSTAR Max DNA polymerase was purchased from Takara; FastDigest *DpnI* was purchased from Thermo Fisher Scientific. NADH, ethyl 2-oxo-4-phenylbutyrate (2a), 2-hydroxy-1-phenylethanone (3a) and 1-phenyl-1,2-ethanediol (3b) were purchased from Aladdin; 4'-chloroacetophenone (1a), 4'-bromoacetophenone (5a), 3'-methoxyacetophenone (6a), 4'-methoxyacetophenone (7a), methyl acetoacetate (8a), ethyl acetoacetate (9a), ethyl-4-chloroacetoacetate (10a), 3-methoxyphenethyl ethanol (6b), 4-methoxyphenethyl ethanol (7b), 1-(4-chlorophenyl) ethanol (1b), 1-(4-bromophenyl) ethanol (5b), methyl 3-hydroxybutyrate (8b), ethyl 3-hydroxybutyrate (9b) and 4-chloro-3-hydroxybutanoate (10b) were purchased from Sigma Aldrich; acetophenone (11a), phenylethanol (11b) and ethyl 2-hydroxy-4-phenylbutyrate (2b) were purchased from TCI (Shanghai) Development Co., Ltd.; 4-fluoroacetophenone (4a) and 1-(4-fluorophenyl) ethanol (4b) were purchased from Alfa Aesar. All other chemicals were analytical grade purity.

### 2.2. Analytical methods of the substrates and chiral alcohols

GC methods. The samples were analyzed by GC analysis (GC 2010, Shimadzu Corp). Use chiral columns HP Chiral 10B, HP Chiral 20% or CP-Chirasil-Dex-CB (Agilent Technologies, China). The methods in detail were described in Table S2.

HPLC method. The 1-phenyl-1,2-ethanediol (PED) and 2-hydroxy-1-phenylethanone (HAP) were analyzed on C18 chromatographic column (XBridge™ C18, 4.6  $\phi$  × 250 mm, 5  $\mu$ m, Waters Technologies (Shanghai) Limited) by using HPLC analysis (Agilent 1260 HPLC). UV detection wavelength of PED and HAP were 215 nm and 245 nm, oven temperature was 35 °C, and sample size was 20  $\mu$ L. The mobile phase was a mixture of water/acetonitrile (v/v, 3/2, 0.1% trifluoroacetic acid in water) and the flow rate was 0.5 mL/min. The retention times of PED (215 nm) and HAP (245 nm) were 6.24 and 7.80 min, respectively. The

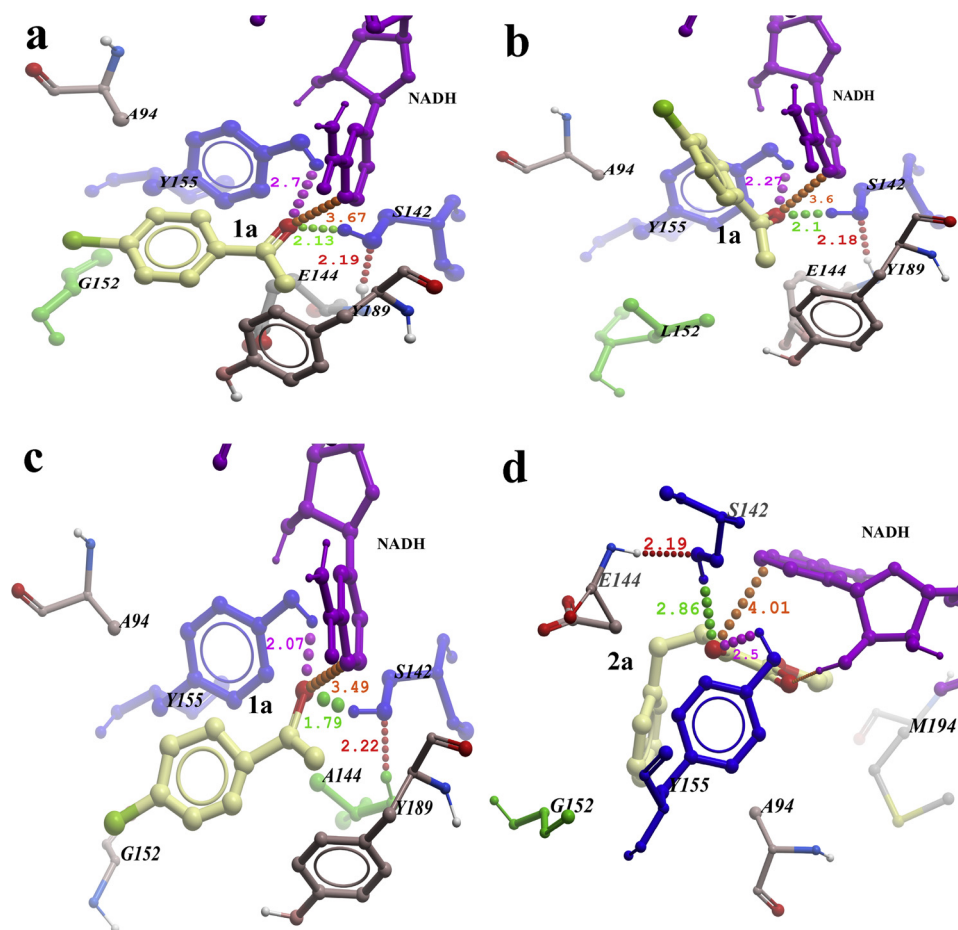


**Fig. 2.** Docking of substrates into the active site of WT and mut-AcCR. Figures showed the amino acid residues of enzyme around substrate, a-c: AcCR, mut-G152 L and mut-E144A docking with 4'-chloro-acetophenone (1a); d-f: AcCR, mut-G152 L and mut-Y189 N docking with ethyl 2-oxo-4-phenylbutyrate (2a); g-i: AcCR, mut-G152 L and mut-I147 V docking with 2-hydroxy-1-phenylethanone (3a)..

configuration of PED was analyzed on chiral column (OB-H, 0.46 cm  $\phi$   $\times$  15 cm) by using normal phase HPLC analysis (Agilent 1100 HPLC). UV detection wavelength of PED was 215 nm, oven temperature was 35 °C, and sample size was 20  $\mu$ L. The mobile phase was a mixture of n-hexane/ isopropanol (v/v, 9/1) and the flow rate was 0.7 mL/min. The retention times of (R)-PED and (S)-PED were 8.51 and 10.21 min.

The calculation methods of the initial reaction rate, the product yield and the *e.e.* value were described in our previous report [34].

### 2.3. Homology modeling and hotspots prediction

The GenBank accession number of the nucleotide sequence of AcCR gene is MF419650. Sequence similarity search was performed with the BLAST program within the Protein Data Bank (PDB). The crystal structures of 4RF2, 1ZJY, 1NXQ and 1ZK3 in complex with NADH were used as templates for 3D analysis of the AcCR structure. The MODELER 9.12 program (<http://www.salilab.org>) was used to construct the relaxed models of AcCR. The model evaluation was conducted using the PROCHECK program [35] and visualization of AcCR model was presented by PyMOL (<http://www.pymol.org>). Hot spots prediction was performed using the HotSpot Wizard 2.0 server.

### 2.4. Site-saturation mutagenesis

The plasmid of pGEX-*accr* which harboring AcCR gene from *Acetobacter* sp. CCTCC M209061 was used for the site-directed mutation. The primers for site-saturation mutagenesis were listed in table S1. Subsequently, a saturation mutagenesis library (containing about 100

independent clones) comprising all 20 natural amino acids was initially constructed by the whole plasmid mutagenic PCR using pGEX-*accr* as template. The resulting plasmid (pGEX-mut-*accr*) was transformed into BL21(DE3) for the expression of mut-AcCRs.

### 2.5. Protein expression and purification

The protein expression and purification methods were referred to our previous reports [33,34].

### 2.6. Activity assay

Enzyme activity of AcCR and its mutant were determined by measuring the decrease in the absorbance of NADH at 340 nm ( $\epsilon = 6.22 \text{ mM}^{-1} \text{ cm}^{-1}$ ) using an UV-vis spectrophotometer (Shinmadzu UV-3010, Japan) at 35 °C for 3 min. The enzymatic reaction catalyzed by AcCR or its mutant was conducted with 0.25 mmol/L NADH, 20 mmol/L substrate, 5  $\mu$ L purified enzyme with an appropriate concentration in 2 mL phosphate buffer (50 mmol/L, pH 6.5). One unit (U) of enzyme was defined as previous report [34].

### 2.7. Molecular docking

NADH-enzyme docking and substrate-enzyme docking were performed using Molsoft ICM-Pro 3.8-3. All the carbonyl compound substrates were docked into the substrate-binding pocket of AcCR-NADH, separately. 3D-coordinates (mol2 files) of substrates and NADH were gained from ZINC database. The molecular docking procedure was

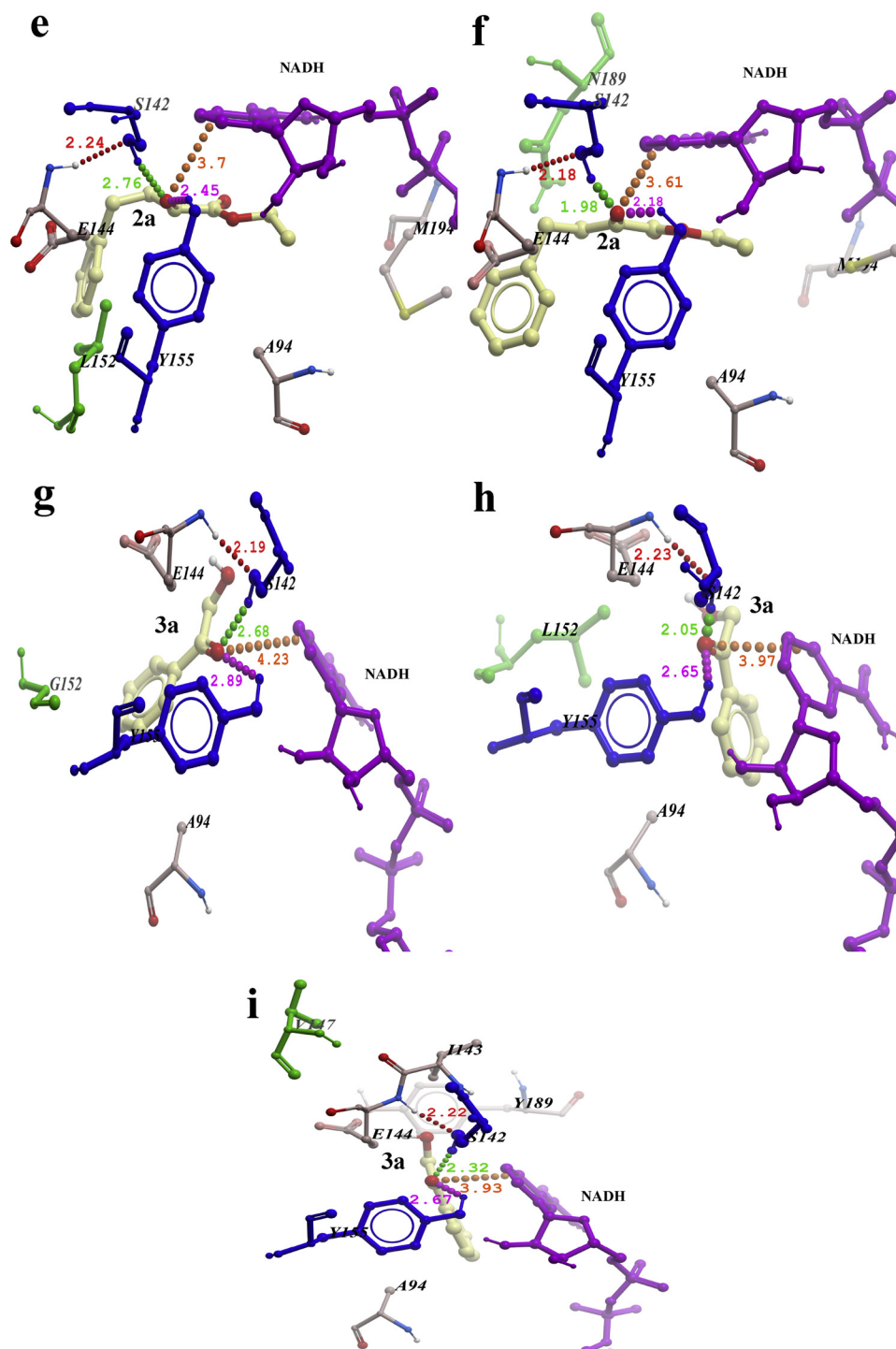


Fig. 2. (continued)

executed by using protocol with the default setting. The molecular docking poses were ranked according to the score functions which were used to predict their binding affinities and conformations of the molecules at the active sites of enzyme [36,37]. Visualization of molecular docking results was presented by LigPlot + v.1.4 and Molsoft ICM-Pro 3.8-3.

### 2.8. Asymmetric bioreduction of carbonyl compounds by AcCR and its variants

Isopropanol was chose to realize the “substrate-coupled” cofactor regeneration system (Figure S5). The reaction were performed in

phosphate buffer (4 mL, 50 mmol/L, pH 6.5) containing 200 mmol/L substrate, 0.1 mmol/L NADH, and 400 mmol/L isopropanol. The reactants were pre-incubated at 35 °C for 10 min, after that a certain amount of AcCR or its mutant was added to start reaction.

## 3. Results and discussion

### 3.1. Molecular modeling

The result of homology modeling was shown in Figure S1. As a short chain dehydrogenase/ reductase, AcCR (Figure S1a) possesses a typical Rossmann structure, which contained the conserved three-dimensional

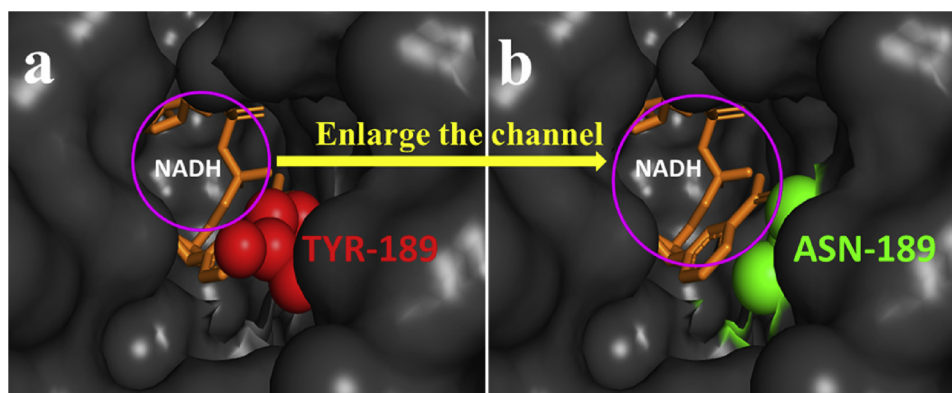


**Fig. 3.** Comparison the substrate channel of AcCR and mut-AcCR (Y189 N). a) the partial view of AcCR (Y189); b) the partial view of mut-AcCR (Y189 N).

**Table 2**

Kinetic parameters of AcCR and its mutants.

Substrate	Mutant	$K_m$ (mM)	$k_{cat}$ ( $s^{-1}$ )	$k_{cat}/K_m$ ( $s^{-1} \text{ mM}^{-1}$ )	Fold change <sup>a</sup>
4'-Chloroacetophenone (1a)	AcCR	$0.3 \pm 0$	$0.5 \times 10^4$	$0.2 \times 10^5$	1.0
	E144A/G 152L	.02	$\pm 62.83$	$1.3 \times 10^6$	65.0
Ethyl 2-oxo-4-phenylbutyrate (2a)	AcCR	$0.12 \pm 0.01$	$1.5 \times 10^5 \pm 148.76$	$1.3 \times 10^4$	1.0
	G152L/Y189N	$0.12 \pm 0.02$	$0.2 \times 10^4 \pm 54.01$	$3.4 \times 10^6$	261.5
2-Hydroxy-1-phenylethanone (3a)	AcCR	$0.05 \pm 0.01$	$1.7 \times 10^5 \pm 88.90$	$2.7 \times 10^3$	1.0
	I147 V/G152L	$0.2 \pm 0.01$	$0.6 \times 10^3 \pm 21.49$	$1.7 \times 10^5$	63.0
		$0.06 \pm 0.01$	$1.0 \times 10^4 \pm 65.48$		

<sup>a</sup> Fold change improvement in  $k_{cat}/K_m$  over the WT enzyme.

**Table 3**

The relative activity of AcCR mutants in reduction of carbonyl compounds.

Substrate	Enzyme activity [U/mg] <sup>a</sup>			
	AcCR	mut-E144A/G152L	mut-G152L/Y189N	mut-I147 V/G152L
4-Chloroacetophenone (1a)	5.17	92.70	2.40	5.12
Ethyl 2-oxo-4-phenylbutyrate (2a)	1.45	1.78	88.96	2.48
2-Hydroxy-1-phenylethanone (3a)	0.37	0.85	1.18	6.44
4-Fluoroacetophenone (4a)	4.40	15.06	0.10	2.39
4-Bromoacetophenone (5a)	6.05	19.57	1.14	4.92
3'-Methoxyacetophenone (6a)	0.55	1.80	0.24	0.26
4'-Methoxyacetophenone (7a)	0.26	1.41	0.06	0.35
Methyl acetoacetate (8a)	4.19	7.68	3.43	32.58
Ethyl acetoacetate (9a)	2.69	2.58	4.83	15.87
Ethyl-4-chloroacetoacetate (10a)	6.24	8.43	3.26	18.71
Acetophenone (11a)	0.48	0.35	0.13	1.71

<sup>a</sup> 0.25 mM NADH, citrate-phosphate bufer (pH 6.5, 50 mM), and 20 mM substrate were incubated at 35 °C for 5 min followed by adding a certain amount of purified enzyme, the changes in absorbance were recorded in 3 min.

structure and active sites (Ser142-Tyr155-Lys159). The 3D structure of AcCR almost overlapped with the reference models (Figure S1b).

As shown in Figure S2, the coenzyme binding pocket of AcCR was broad and the NADH molecule was bounded to AcCR with an extended conformation at carbonyl ends of the central parallel  $\beta$ -sheet, whose nicotinamide ring located at the bottom of the lobe region. This orientation was beneficial to deliver NADH-C4 hydride of the nicotinamide ring to the carbonyl carbon of the substrate bond in the lobe region. Moreover, the conserved coenzyme binding motif Gly13-xxx-Gly17-x-Gly19 and catalytic active sites (Ser142 and Tyr159) were

located near the NADH molecule (Figure S2b). There existed hydrogen-bond interactions between amino acid residues (Ile18, Gly19, Tyr 155 and Ile190) and the pyrophosphate part of NADH, which could increase the stability of AcCR-NADH interaction [38]. Moreover, it has been suggested that Ser142 could provide stable interaction to stabilize the substrate or reaction intermediate through a hydrogen-bond [36]. Tyr155 acted as a general base for initiating the catalysis by transferring proton to the substrate carbonyl from NADH-C4 [39,40].

### 3.2. Exploring key residues of AcCR by hotspot prediction

To improve the catalytic efficiency of the AcCR, mutational hot spots in the AcCR amino acid sequence were analyzed by using the HotSpot Wizard2.0 server [41]. Seven hot spot residues (Ala94, Ser96, Glu144, Met151, Gly152, Ala153, Trp191) were identified (Figure S3a), and the hot spots were located near the catalytic active sites or the channel of substrates/products in and out of the AcCR (Figure S3b). In addition, Ile147 as mutation site was transformed to Val for investigating the influence of Ile and Val, owing to the contribution of hydrophobic interactions of Val and Ile on protein surface [42,43]. Moreover, Tyr189 was bulky aromatic amino acid and locate at the entrance of AcCR active center (Fig. 3), which may hinder the substrates get in and out of the AcCR active center. Therefore, the aforementioned nine residues were identified and altered by site-saturated mutagenesis (Fig. 1) to obtain mutants of AcCR (mut-AcCR).

### 3.3. Analysis of the activity improvement of most active mutants

The specific activities of the purified mut-AcCRs to three aromatic ketones (aromatic ketone ester) were determined by measuring the absorbance decrease of NADH in 2 mL reaction system. The results of effective mut-AcCRs were summarized in Table 1. As shown in Table 1, the mut-G152L was considerably more active with 4.0–11.6 folds improved activity than WT AcCR. For the best substrate (4'-

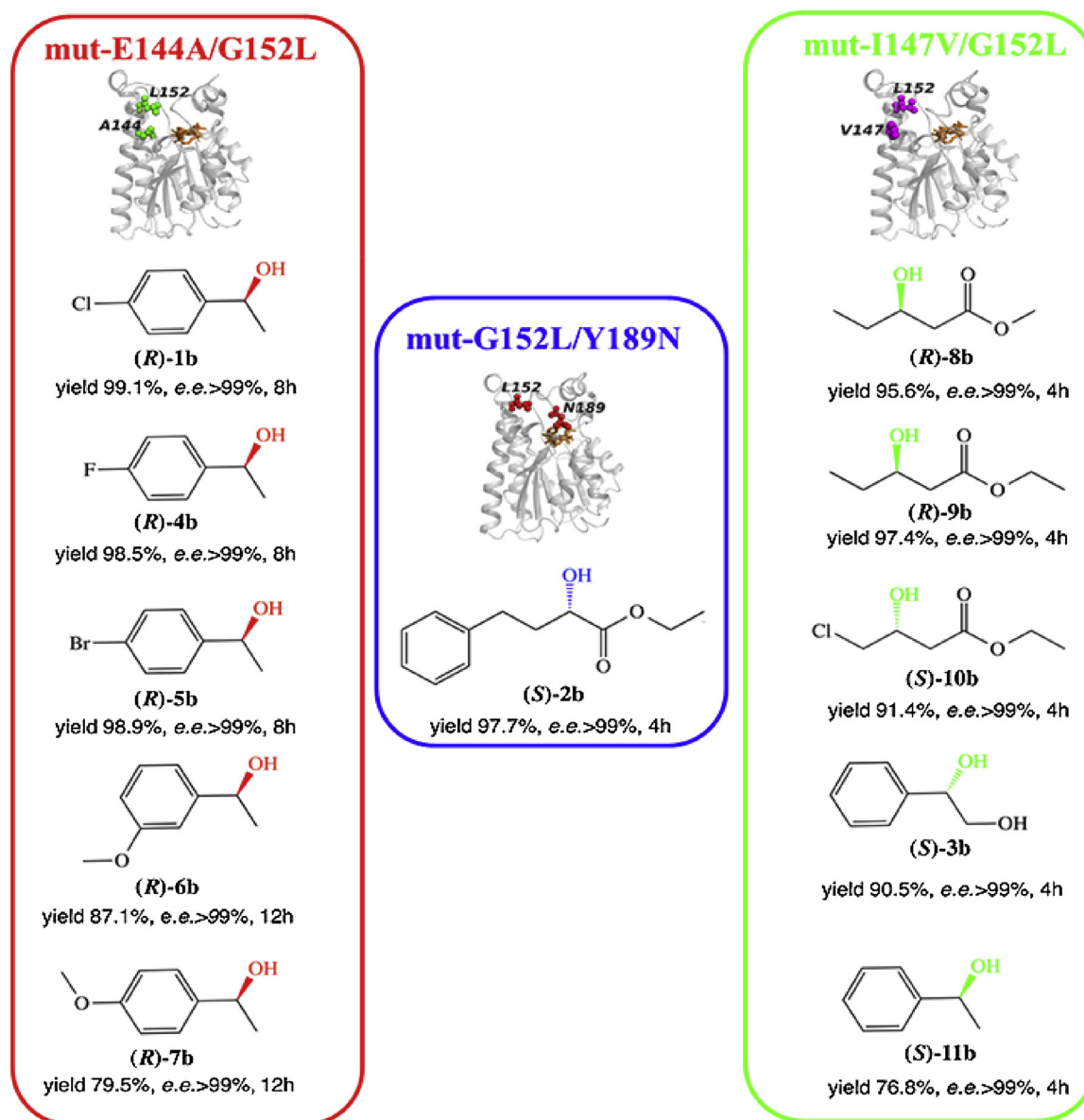


Fig. 4. Asymmetric reduction of prochiral substrates catalyzed by AcCR mutants. Phosphate buffer (pH 6.5, 50 mmol/L, 4 mL) containing 200 mmol/L substrate, 0.1 mmol/L NADH, and 400 mmol/L isopropanol, 35 °C, 200 rpm, 1 mg AcCR mutant.

chloroacetophenone, 1a) of mut-E144A, the specific activity of mut-E144A was further increased to 47.2 U/mg, which was 9.1 folds higher than that of the WT AcCR. Meanwhile, for the aromatic ketone ester substrate (ethyl 2-oxo-4-phenylbutyrate, 2a), the specific activity of mut-Y189N was enormously enhanced to 73.4 U/mg, which was 50.6 folds higher than that of WT one. Additionally, with the difficult-to-reduce ketone catalyzed by WT AcCR, the specific activity of WT AcCR to 2-hydroxy-1-phenylethanone (3a) was only 0.4 U/mg. Notably, the specific activity of mut-G152L to the same substrate could reach to 4.3 U/mg, which was 11.6 folds higher than that of the WT one.

### 3.4. Molecular docking analysis

For the sake of understanding the structural basis of the striking increase in the specific activity of mut-AcCRs towards the three substrates, the ketones 1a, 2a and 3a were docking into the substrate-binding pocket of WT AcCR and its mutants, respectively. Such an analysis would be useful for understanding the increased specific activity of mut-AcCRs. Three residues (Ser 142, Tyr 155 and Lys 159)

were proposed as the catalytic triad in the carbonyl reductase AcCR. The carbonyl oxygen atom of substrate formed hydrogen bonds with Ser142 and Tyr 155 residues, and was protonated from the C4-H atom of NADH [44,45]. The overlay of the lowest energy docked conformations of the three substrates into the enzyme active site were shown in Fig. 2. The most possible conformations of 1a, 2a and 3a in the active sites of AcCR and mut-G152L were obtained (Fig. 2a, 2b, 2d, 2e, 2g, 2h). As shown in Fig. 2a and b, the distances between the oxygen atoms of the carbonyl group of 1a and Tyr155 were 2.7 Å and 2.27 Å, respectively. The distance was shortened by 0.43 Å in the two dockings, which could possibly increase the protonation of oxygen atom of 1a, resulting in the improvement of the specific activity of mut-G152L, as well as the consequence of other two substrates [46]. When the amino acid residue Glu at site of 144 was mutated to Ala (Fig. 2a and 2c), the distance in the two dockings between Glu/Ala and oxygen atom of 1a was shortened by 0.63 Å, which could also increase the protonation, and the distance between oxygen atom of 1a and amino acid residue 142Ser was shortened by 0.4 Å, which could increase the stability of enzyme-substrate complex.

Compared the result of 2a docking with WT AcCR (4.01 Å), the

distances between the oxygen atoms of the carbonyl groups of 2a and C4-H of nicotinamide mononucleotide (NMN) of cofactor were decreased obviously (3.7 and 3.61 Å) (Fig. 2d–f), due to the substrate of 2a docking with mut-G152L and mut-Y189N. The shorter distance suggested a faster hydrogen transfer process which delivered from C4 of NMN to oxygen atom and improved the specific activity of mut-G152L and Y189N to 2a [47]. Importantly, it was worth noting that the Tyr189 was bulky aromatic amino acid and located at the channel of the enzyme active center which could interfere with the larger compounds of 2a and 2b in and out of the active center [48].

As shown in Fig. 3, the replacement of Tyr to Asn at the 189 site (Asn as a smaller amino acid with similar character of Tyr) could enlarge the channel and gave a rise to 50.58 folds enhancement of the specific activity, which combined with the distances diminution between 2a and C4-H of NMN, Tyr155 and Ser142, respectively. The docking results of WT AcCR, mut-I147V and mut-G152L with substrate of 3a were shown in Fig. 2g–i. From the docking results, it could be observed that the residues Ser142 forms hydrogen bond with the oxygen atom of 3a, the distances between the two atoms were 2.68 Å (WT AcCR), 2.05 Å (mut-G152L) and 2.32 Å (mut-I147V), respectively. The Ser142 as active site in carbonyl reductase was deemed to stabilize the substrate and reaction intermediate through a hydrogen bond [36,49]. The decrease of the distances caused the improvement of the hydrogen-bond interaction between Ser142 and oxygen atom of 3a, and further increased the stability of substrate-enzyme complex, which could promote the enhancement of the specific activity of the two mut-AcCRs towards 3a.

The specific activities of AcCR (mut-G152L) towards different substrates (1a, 2a, 3a) were significantly improved after the mutation of Gly152 to Leu152. Moreover, the specific activity of mut-E144A to 1a, mut-Y189N to 2a, mut-I147V to 3a, mut-W191A to 3a and mut-M151T to 3a have been improved to varying degrees from 3.7 to 50.6 folds (Table 1). Therefore, the combination of mutated site Leu152 and others were conducted to obtain double-mutants. Finally, Five double-mutants, mut-E144A/G152L, mut-G152L/Y189N, mut-M151T/G152L, mut-I147V/G152L and mut-G152L/W191A, were achieved. Among them, the specific activity of the double-mutant mut-E144A/G152L to the substrate 1a reached to 92.7 U/mg, which was 17.9 folds higher than that of WT AcCR (5.2 U/mg), indicating a dramatic improvement of the specific activity. For the substrate 2a, the specific activity of mut-G152L/Y189N increased to 88.9 U/mg, which was 61.3 folds higher than that of WT AcCR (1.5 U/mg). Additionally, substrate of 3a as an important prochiral carbonyl compound has been used to test the activity of the mut-AcCRs. The specific activity of mut-M151T/G152L, mut-I147V/G152L and mut-G152L/W191A were enhanced by 13.9, 17.4 and 14.5 folds, respectively. Furthermore, the dockings of the double-mutant mut-AcCRs with different substrates were shown in Figure S4.

The shortened distances between the substrates and C4-H of NMN, as well as the substrates and the catalytic sites Tyr155/ Ser142, enhanced the hydrogen-bond interactions in substrate-enzyme complexes, promoting the increase of the protonation and H-transfer rates to the oxygen atoms, as well as the stability of the substrate or reaction intermediate through a hydrogen-bond [50].

### 3.5. Kinetic studies

The kinetic parameters of the AcCR and its mutants were calculated by nonlinear regression on the basis of the Michaelis-Menten equation using OriginPro software. All the kinetic constants of the Wt enzyme and mutants towards 1a, 2a and 3a were presented in Table 2. Compared with the WT one, all three mutants had lower  $K_m$  and higher  $k_{cat}$ , indicating the increase of the catalytic efficiency ( $k_{cat}/K_m$ ). The obvious decrease in  $K_m$  confirmed that the binding of variants and substrate were much stronger than the WT one. Among them, variant G152L/Y189N displayed a decrease in  $K_m$  and 850-fold increase in  $k_{cat}$ , which

led to a 261-fold improvement in the catalytic efficiency.

### 3.6. Biocatalytic reduction of various substrates using the AcCR mutants

A series of substrates (1a–11a) with a wide range of structure features was applied to characterize the substrate specificity of the mutants. As shown in Table 3, the specific activities of mut-E144A/G152L towards 4'-halogenated acetophenones were 15.1, 92.7 and 19.6 U/mg, respectively, which have improved 3.3–17.9 folds. For 3'- and 4'-methoxy substituted acetophenone, the specific activity have been enhanced 3.3- and 5.4-fold, respectively, which were obviously higher than that of WT AcCR. The specific activities of mut-I147V/G152L towards  $\beta$ -aliphatic ketone ester and acetophenone have been raised 3.0–7.8 folds. In all the 11 tested substrates, two of the double-mutants (mut-E144A/G152L for 1a and mut-G152L/Y189N for 2a) have been improved remarkably with the specific activities more than 88 U/mg.

The asymmetric reductions of various prochiral substrates catalyzed by the AcCR double-mutants (mut-E144A/G152L, mut-G152L/Y189N and mut-I147V/G152L) have been conducted with 200 mM different substrates and regeneration of NADH through oxidation of isopropanol (Figure S6). The results were summarized in Fig. 4. In our previous study [34], the wild type AcCR could only catalyze the asymmetric reduction of 50 mmol/L substrates, and the product yields were low (10.8–66.9%) to most of the investigated substrates except 4'-halogenated acetophenones. The modified mut-AcCRs exhibited outstanding activity for bioreduction of different substrates with gratifying product yields ranged from 76.8% to 99.1% as well as excellent *e.e.* value (> 99%), which were much more improvement than that of WT one. The satisfactory results of the bioreduction reaction catalyzed by mut-AcCRs gave a promising strategy for the synthesis of chiral alcohols in higher substrate concentrations of various prochiral carbonyl compounds.

## 4. Conclusions

In conclusion, the specific activity of anti-Prelog carbonyl reductase AcCR from *Acetobacter* sp. has been significantly enhanced by site-directed mutations combined with double-mutants. The improvement of specific activity of the mut-AcCRs is attributed to the enhancement of hydrogen-bond interaction and the promotion of protonation and hydrogen transfer rate. By using various of prochiral carbonyl compounds at high concentration as substrates, the resultant mut-AcCRs are successfully employed for efficient synthesis of enantiomerically pure chiral alcohols with product yields ranged from 76.8%–99.1% and *e.e.* value more than 99%, indicating that the mut-AcCRs are potential for further catalytic applications.

### Declaration of Competing Interest

None.

### Acknowledgements

The authors gratefully acknowledged the National Natural Science Foundation of China (No. 21676104 and 21878105), the National Key Research and Development Program of China (2018YFC1602100, 2018YFC1603400), the Key Research and Development Program of Guangdong Province (No. 2019B020213001), and the Science and Technology Program of Guangzhou (201904010360) for partially funding this work.

### Appendix A. Supplementary data

Supplementary material related to this article can be found, in the online version, at doi:<https://doi.org/10.1016/j.mcat.2019.110613>.

## References

- [1] J.A. Kelly, M. Giese, K.E. Shopsowitz, W.Y. Hamad, M.J. MacLachlan, The development of chiral nematic mesoporous materials, *Accounts Chem. Res.* 47 (2014) 1088–1096.
- [2] Y. Ni, J.H. Xu, Biocatalytic ketone reduction: a green and efficient access to enantiopure alcohols, *Biotechnol. Adv.* 30 (2012) 1279–1288.
- [3] M.H. Uzir, N. Najimudin, On the bi-enzymatic behaviour of *Saccharomyces cerevisiae*-mediated stereoselective biotransformation of 2,6,6-trimethylcyclohex-2-ene-1,4-dione, *Mol. Catal.* 447 (2018) 56–64.
- [4] G.W. Zheng, Y.Y. Liu, Q. Chen, L. Huang, H.L. Yu, W.Y. Lou, C.X. Li, Y.P. Bai, A.T. Li, J.H. Xu, Preparation of structurally diverse chiral alcohols by engineering ketoreductase CgKR, *ACS Catal.* 7 (2017) 7174–7181.
- [5] Y.G. Zheng, H.H. Yin, D.F. Yu, X. Chen, X.L. Tang, X.J. Zhang, Y.P. Xue, Y.J. Wang, Z.Q. Liu, Recent advances in biotechnological applications of alcohol dehydrogenases, *Appl. Microbiol. Biot.* 101 (2017) 987–1001.
- [6] Y.P. Shang, Q. Chen, X.D. Kong, Y.J. Zhang, J.H. Xu, H.L. Yu, Efficient Synthesis of (R)-2-Chloro-1-(2,4-dichlorophenyl)ethanol with a Ketoreductase from *Scheffersomyces stipitis* CBS 6045, *Adv. Synth. Catal.* 359 (2017) 426–431.
- [7] B. Lin, Y. Tao, Whole-cell biocatalysts by design, *Microb. Cell Fact.* 16 (2017) 106.
- [8] K. Wu, H. Wang, L. Chen, H. Fan, Z. Zhao, D. Wei, Practical two-step synthesis of enantiopure styrene oxide through an optimized chemoenzymatic approach, *Appl. Microbiol. Biot.* 100 (2016) 8757–8767.
- [9] N. Itoh, Use of the anti-Prelog stereoselective alcohol dehydrogenase from *Leifsonia* and *Pseudomonas* for producing chiral alcohols, *Appl. Microbiol. Biot.* 98 (2014) 3889–3904.
- [10] W.G. Birolli, I.M. Ferreira, N. Alvarenga, D.A. Santos, I.L. de Matos, J.V. Comasseto, A.L.M. Porto, Biocatalysis and biotransformation in Brazil: An overview, *Biotechnol. Adv.* 33 (2015) 481–510.
- [11] M.M. Musa, R.S. Phillips, Recent advances in alcohol dehydrogenase-catalyzed asymmetric production of hydrophobic alcohols, *Catal. Sci. Technol.* 1 (2011) 1311–1323.
- [12] G.C. Xu, H.L. Yu, X.Y. Zhang, J.H. Xu, Access to optically active aryl halohydrins using a substrate-tolerant carbonyl reductase discovered from *Kluyveromyces thermotolerans*, *ACS Catal.* 2 (2012) 2566–2571.
- [13] G.V. Dhoke, C. Loderer, M.D. Davari, M. Ansorge-Schumacher, U. Schwaneberg, M. Bocla, Activity prediction of substrates in NADH-dependent carbonyl reductase by docking requires catalytic constraints and charge parameterization of catalytic zinc environment, *Aid. Mol. Des.* 29 (2015) 1057–1069.
- [14] Z. Sun, R. Lonsdale, A. Ilie, G. Li, J. Zhou, M.T. Reetz, Catalytic asymmetric reduction of difficult-to-reduce ketones: triple-code saturation mutagenesis of an alcohol dehydrogenase, *ACS Catal.* 6 (2016) 1598–1605.
- [15] H. Groger, W. Hummel, C. Rollmann, F. Chamouleau, H. Husken, H. Werner, C. Wunderlich, K. Abokitse, K. Drauz, S. Buchholz, Preparative asymmetric reduction of ketones in a biphasic medium with an (S)-alcohol dehydrogenase under in situ-cofactor-recycling with a formate dehydrogenase, *Tetrahedron.* 60 (2004) 633–640.
- [16] G. De Gonzalo, I. Lavandera, K. Durchschein, D. Wurm, K. Faber, W. Kroutil, Asymmetric biocatalytic reduction of ketones using hydroxy-functionalised water-miscible ionic liquids as solvents, *Tetrahedron-Asym.* 18 (2007) 2541–2546.
- [17] R.Z. Zhang, Y. Xu, R. Xiao, Redesigning alcohol dehydrogenases/reductases for more efficient biosynthesis of enantiopure isomers, *Biotechnol. Adv.* 33 (2015) 1671–1684.
- [18] Q. Chen, Z.J. Luan, H.L. Yu, X. Cheng, J.H. Xu, Rational design of a carboxylic esterase *RhEst1* based on computational analysis of substrate binding, *J. Mol. Graph. Model.* 62 (2015) 319–324.
- [19] Y.J. Wang, B.B. Ying, W. Shen, R.C. Zheng, Y.G. Zheng, Rational design of *Kluyveromyces marxianus* ZJB14056 aldo-keto reductase *KmAKR* to enhance diastereoselectivity and activity, *Enzyme Microb. Tech.* 107 (2017) 32–40.
- [20] Y. Nie, Y. Xu, X.Q. Mu, H.Y. Wang, M. Yang, R. Xiao, Purification, characterization, gene cloning, and expression of a novel alcohol dehydrogenase with anti-prelog stereospecificity from *Candida parapsilosis*, *Appl. Environ. Microb.* 73 (2007) 3759–3764.
- [21] Y. Nie, R. Xiao, Y. Xu, G.T. Montelione, Novel anti-Prelog stereospecific carbonyl reductases from *Candida parapsilosis* for asymmetric reduction of prochiral ketones, *Org. Biomol. Chem.* 9 (2011) 4070–4078.
- [22] R.Z. Zhang, Y. Xu, Y. Sun, W.C. Zhang, R. Xiao, Ser67Asp and His68Asp substitutions in *Candida parapsilosis* carbonyl reductase alter the coenzyme specificity and enantioselectivity of ketone reduction, *Appl. Environ. Microb.* 75 (2009) 2176–2183.
- [23] R.Z. Zhang, Y.W. Geng, Y. Xu, W. Zhang, S. Wang, R. Xiao, Carbonyl reductase SCRII from *Candida parapsilosis* catalyzes anti-Prelog reaction to (S)-1-phenyl-1,2-ethanediol with absolute stereochemical selectivity, *Bioresour. Technol.* 102 (2011) 483–489.
- [24] N. Richter, W. Hummel, Biochemical characterisation of a NADPH-dependent carbonyl reductase from *Neurospora crassa* reducing alpha- and beta-keto esters, *Enzyme Microb. Tec.* 48 (2011) 472–479.
- [25] G.W. Zheng, J.H. Xu, New opportunities for biocatalysis: driving the synthesis of chiral chemicals, *Curr. Opin. Biotechnol.* 22 (2011) 784–792.
- [26] M.D. Truppo, Biocatalysis in the pharmaceutical industry, *ACS Med. Chem. Lett.* 8 (2017) 476–480.
- [27] F. Qin, B. Qin, T. Mori, Y. Wang, L. Meng, X. Zhang, X. Jia, I. Abe, S. You, Engineering of *Candida glabrata* ketoreductase 1 for asymmetric reduction of  $\alpha$ -Halo ketones, *ACS Catal.* 6 (2016) 6135–6140.
- [28] C.M. Nealon, M.M. Musa, J.M. Patel, R.S. Phillips, Controlling substrate specificity and stereospecificity of alcohol dehydrogenases, *ACS Catal.* 5 (2015) 2100–2114.
- [29] M.M. Musa, N. Lott, M. Laivenieks, L. Watanabe, C. Vieille, R.S. Phillips, A single point mutation reverses the enantiopreference of thermoaerobacter ethanolicus secondary alcohol dehydrogenase, *ChemCatChem.* 1 (2009) 89–93.
- [30] K. Honda, M. Inoue, T. Ono, K. Okano, Y. Dekishima, H. Kawabata, Expression of engineered carbonyl reductase from *Ogataea minuta* in *Rhodococcus opacus* and its application to whole-cell bioconversion in anhydrous solvents, *J. Biosci. Bioeng.* 123 (2017) 673–678.
- [31] X. Luo, Y.J. Wang, W. Shen, Y.G. Zheng, Activity improvement of a *Kluyveromyces lactis* aldo-keto reductase *KIAKR* via rational design, *J. Biotechnol.* 224 (2016) 20–26.
- [32] P. Wei, J. Liang, J. Cheng, M.H. Zong, W.Y. Lou, Markedly improving asymmetric oxidation of 1-(4-methoxyphenyl) ethanol with *Acetobacter* sp. CCTCC M209061 cells by adding deep eutectic solvent in a two phase system, *Microb. Cell Fact.* 15 (2016) 5.
- [33] P. Wei, J.X. Gao, G.W. Zheng, H. Wu, M.H. Zong, W.Y. Lou, Engineering of a novel carbonyl reductase with coenzyme regeneration in *E. Coli* for efficient biosynthesis of enantiopure chiral alcohols, *J. Biotechnol.* 230 (2016) 54–62.
- [34] P. Wei, Y.H. Cui, M.H. Zong, P. Xu, J. Zhou, W.Y. Lou, Enzymatic characterization of a recombinant carbonyl reductase from *Acetobacter* sp. CCTCC M209061, *Bioresour. and Bioproc.* 4 (2017) 39.
- [35] R.A. Laskowski, M.W. Macarthur, D.S. Moss, J.M. Thornton, PROCHECK: a program to check the stereochemical quality of protein structures, *J. Appl. Crystallogr.* 26 (1993) 283–291.
- [36] J. Deng, Z. Yao, K. Chen, Y.A. Yuan, J. Lin, D. Wei, Towards the computational design and engineering of enzyme enantioselectivity: a case study by a carbonyl reductase from *Glucobacter oxydans*, *J. Biotechnol.* 217 (2016) 31–40.
- [37] D.L. Zhang, X. Chen, J. Chi, J.H. Feng, Q.Q. Wu, D.M. Zhu, Semi-rational engineering a carbonyl reductase for the enantioselective reduction of beta-amino ketones, *ACS Catal.* 5 (2015) 2452–2457.
- [38] A.M. Lesk, NAD-binding domains of dehydrogenases, *Curr. Opin. Struc. Biol.* 5 (1995) 775–783.
- [39] K.L. Kavanagh, H. Jornvall, B. Persson, U. Oppermann, Medium- and short-chain dehydrogenase/reductase gene and protein families: the SDR superfamily: functional and structural diversity within a family of metabolic and regulatory enzymes, *Cell. Mol. Life Sci.* 65 (2008) 3895–3906.
- [40] D.J. Hosfield, Y.Q. Wu, R.J. Skene, M. Hilgers, A. Jennings, G.P. Snell, K. Aertgeerts, Conformational flexibility in crystal structures of human 11 beta-hydroxysteroid dehydrogenase type I provide insights into glucocorticoid interconversion and enzyme regulation, *J. Biol. Chem.* 280 (2005) 4639–4648.
- [41] H. Jochens, U.T. Bornscheuer, Natural diversity to guide focused directed evolution, *ChemBioChem.* 11 (2010) 1861–1866.
- [42] Y. Sugita, A. Kitao, N. Go, Computational analysis of thermal stability: effect of Ile $\rightarrow$ Val mutations in human lysozyme, *Fold. Des.* 3 (1998) 173–181.
- [43] S.M. Weisslocker, M. Lembrouk, J. Santolini, P. Dorlet, Revisiting the Val/Ile mutation in mammalian and bacterial nitric oxide synthases: a spectroscopic and kinetic study, *Biochemistry.* 56 (2017) 748–756.
- [44] D.M. Zhu, L. Hua, Enantioselective enzymatic reductions of sterically bulky aryl alkyl ketones catalyzed by a NADPH-Dependent carbonyl reductase, *J. Org. Chem.* 71 (2006) 9484–9486.
- [45] S. Kamitori, A. Iguchi, A. Ohtaki, M. Yamada, K. Kita, X-ray structures of NADPH-dependent carbonyl reductase from *Sporobolomyces salmonicolor* provide insights into stereoselective reductions of carbonyl compounds, *J. Mol. Biol.* 352 (2005) 551–558.
- [46] K.R. Beck, T. Kaserer, D. Schuster, A. Odermatt, Virtual screening applications in short-chain dehydrogenase/reductase research, *J. Steroid Biochem. Mol. Biol.* 171 (2017) 157–177.
- [47] X. Chen, H. Zhang, J. Feng, Q. Wu, D.M. Zhu, Molecular basis for the high activity and enantioselectivity of the carbonyl reductase from *Sporobolomyces salmonicolor* toward  $\alpha$ -Haloacetophenones, *ACS Catal.* 8 (2018) 3525–3531.
- [48] M. Li, Z.J. Zhang, X.D. Kong, H.L. Yu, J.H. Zhou, J.H. Xu, Engineering *Streptomyces coelicolor* carbonyl reductase for efficient atorvastatin precursor synthesis, *Appl. Environ. Microb.* 83 (2017) 603–617.
- [49] C. Filling, K.D. Berndt, J. Benach, S. Knapp, T. Prozorovskii, E. Nordling, R. Ladenstein, H. Jörnvall, U. Oppermann, Critical residues for structure and catalysis in short-chain Dehydrogenases/Reductases, *J. Biol. Chem.* 277 (2002) 25677–25684.
- [50] R. Ladenstein, J.-O. Winberg, J. Benach, Structure-function relationships in short-chain alcohol dehydrogenases, *Cell. Mol. Life Sci.* 65 (2008) 3918–3935.